



Review in Advance first posted online  
on January 30, 2012. (Changes may  
still occur before final publication  
online and in print.)

# Ultrathin Oxide Films on Metal Supports: Structure-Reactivity Relations

S. Shaikhutdinov and H.-J. Freund

Fritz Haber Institute of the Max Planck Society, 14195 Berlin, Germany;  
email: shaikhutdinov@fhi-berlin.mpg.de, freund@fhi-berlin.mpg.de

Annu. Rev. Phys. Chem. 2012. 63:27.1–27.15

The *Annual Review of Physical Chemistry* is online at  
physchem.annualreviews.org

This article's doi:  
10.1146/annurev-physchem-032511-143737

Copyright © 2012 by Annual Reviews.  
All rights reserved

0066-426X/12/0505-0001\$20.00

## Keywords

heterogeneous catalysis, ultrathin oxide layers, model systems, surface structure

## Abstract

Well-ordered, thin oxide films have drawn some attention in recent years as suitable oxide supports for modeling highly dispersed metal catalysts at the atomic scale. It turned out, however, that ultrathin oxide films may exhibit interesting catalytic properties in their own right. In this review, we discuss phenomena specifically connected to ultrathin oxide films to explain and understand the physicochemical basis of their reactivity in oxidation reactions. Two sets of systems are discussed, i.e., transition metal oxide films grown on metal substrates and native oxide films formed upon oxidation of metal surfaces.

**UHV:** ultrahigh vacuum

## INTRODUCTION

Well-ordered, thin oxide films have drawn some attention in recent years as a means to study dispersed metal catalysts at the atomic scale (1–3). Their study has contributed considerably to our understanding of such systems, as they allow us to reduce the complexity of the real system and yet capture—in contrast to metal single crystals—an important part of it, in particular, the finite size, and thus the flexibility of the system, and the metal/oxide interface. The latter aspects turn out to be decisive, in many cases, for a detailed understanding of nanoscaled systems as they are represented by dispersed metal catalysts. When prepared in ultrahigh vacuum (UHV) and under reproducible conditions, much may be learned about the thermodynamic stability of thin oxide films (4) and, concomitantly, about adsorption and reaction on those systems, with respect to the relation between geometric and electronic structures as well as to reaction kinetics (5, 6). The relation between the information gained and the results of catalytic studies under ambient conditions should be carefully evaluated on a case-to-case basis. One important aspect is to know whether the system changes considerably under the applied reaction conditions. As an example, consider oxidation reactions where the system is exposed to higher doses or pressure of oxygen together with considerable changes in temperature. As a consequence, the supported metal particles may be totally or partially oxidized, and also the state of the support may undergo substantial changes. Such changes have recently been documented and have led to the investigation of ultrathin oxide films from a different perspective (2), which is the exclusive topic of this review. Let us explain what we mean by considering a few examples reported in the literature.

As a first example, we consider the so-called strong metal-support interaction (SMSI), which for many years has been known to occur when a dispersed metal catalyst on a reducible oxide support is heated above a threshold temperature in a reducing atmosphere (7–12). In most cases, the SMSI effect has been assigned to the migration of an oxide layer from the support onto the metal particles, rendering those practically unreactive because the oxide suppresses adsorption of molecules otherwise readily adsorbing on a metal surface. The migrating oxide covers the metal particle as an ultrathin oxide film whose stoichiometry and structure, again, is often not well known (13, 14). Certainly, the SMSI state depends on the metal, the oxide, and the reaction. Nevertheless, it is believed that the encapsulation will deactivate all—and in particular, structure-sensitive—reactions on metals. But one may raise the question, Is this always true? Indeed, the previous statement implies that the encapsulated oxide layer is inert in the reaction and remains unchanged, which is not obvious in the case of ultrathin films because their structural and chemical properties are often considerably different from the bulk counterparts (15).

As a second set of examples, we address the recent and still ongoing debates on CO oxidation on platinum group metals (Pt, Pd, etc.), and on Ru, in particular, which was found to be the least reactive under UHV conditions but the most reactive at technologically relevant (i.e., atmospheric) pressures (16–24). Here, it was demonstrated that under reaction conditions the metal surface was covered by an oxidic layer, which originally was thought to represent a dense ( $1 \times 1$ ) phase of chemisorbed oxygen, and later even a stoichiometric  $\text{RuO}_2(110)$  film. Through a controversial interplay between experiment and theory, it is now believed that the active phase is neither a chemisorbed oxygen phase nor the stoichiometric  $\text{RuO}_2(110)$  phase but rather a very thin ruthenium oxide film of not yet well-determined structure.

Of course, oxygen-induced restructuring of oxide-supported metal nanoparticles may proceed along different routes, which does not necessarily lead to well-defined oxide overlayers but rather to ill-defined oxide phases at the metal/support interface (25). An example where this has been studied and the spatial confinements of the metal oxide phase in/on the particle to the particle/support

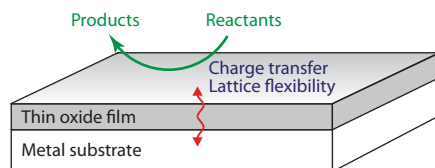


**Figure 1**

Schematic representation of an ultrathin oxide film, grown on a metal, reacting with ambient gases through charge transfer to adsorbed species accompanied by lattice distortion.

interface has been proven is the case of a Pd/Fe<sub>3</sub>O<sub>4</sub>(111) model system (26). This topic is beyond the scope of this review and is not further discussed.

In this review, we discuss only phenomena specifically connected to ultrathin oxide films to explain the physicochemical basis of their reactivity, which can be traced to some very old ideas discussed in the late 1940s.

## GENERAL IDEAS

**Figure 1** shows a very simple schematic of the situation we are considering. An ultrathin film is placed onto a metallic substrate. Although simplified in the figure, the structure of the ultrathin film, which is determined by the epitaxial relation to the metal substrate, plays an important role in determining its properties, as discussed below.

To analyze the situation with the help of simple physical models, one has to consider the physical quantities that determine electron transfer, e.g., from the metal substrate through the film toward a species located on the film surface. On the one hand, there is the ionization potential required to excite an electron from the metal oxide, which is, in general, not simply the work function of the metal but a related quantity, because it will be substantially modified by the presence of the oxide overlayer. On the other hand, there is the electron affinity of the species adsorbed on the oxide surface, which again may be influenced by the interaction with the oxide surfaces and hence be different from the isolated species. If the energy balance between these quantities results in an energy gain, then the electron transfer is possible, in principle. However, this is only part of a proper description because it is not evident how the process will depend on the thickness of the film, as the energy balance is only weakly dependent on it, and tunneling is possible as long as the film is sufficiently thin. Of course, in the case of thicker films of several nanometers, the tunneling probability, which decays exponentially with thickness, would simply be zero. But why would an oxide film of three layers differ fundamentally from one of, say, eight layers with respect to the process? The reason is connected with the degree of lattice flexibility of oxide films, and at this point the structural aspect comes into play. The lattice flexibility is, of course, directly connected with the phonon spectrum of the film, and the latter is altered very rapidly as the film gets thicker, quickly approaching the phonon behavior of the bulk or a bulk terminating surface (27). Oxides are stiff materials compared with metals, and the energy needed to deform the lattice is relatively large. The situation changes when the oxide in the form of a thin layer is placed onto a metal surface. The metal surface helps to ease the deformation of the lattice upon perturbation. This implies that a thin film has the ability to accommodate the charge accumulated through electron transfer at a species on the film's surface by a lattice distortion, a property that a thick film may not exhibit. The physical phenomenon is called a polaronic distortion (28) and is known from semiconductor physics.

**STM:** scanning tunneling microscopy

One may use this knowledge to choose combinations of materials in thin oxide film design to produce systems with specific electronic properties with respect to electron transfer, which may in turn lead to specific chemical reactivity. Take, e.g., cations, anions, or neutrals of one and the same element adsorbed at a surface: They show different adsorption behavior and hence will undergo very different chemical reactions! Therefore, if we succeed in designing specific support systems that promote the formation of specific charge states, we might reach the point where we design catalysts for specific reactions. Of course, under reaction conditions, the situation is a bit more involved because one has to consider the presence of the gas phase as well when trying to control the electron transfer by materials design. Clearly, the gas phase determines the chemical potential of a catalyst and thus the free energy balance. It is now evident that the phenomenon described is a manifestation of the system's flexibility.

The way the process has been described so far is very similar to the ideas put forward by Cabrera and Mott in 1948 when they discussed the oxidation of metals (29). They assumed that although a semiconducting oxide grows on a metal, the ability to transfer electrons to adsorbed oxygen, forming a negatively charged species, leads to an electric field that provides the driving force for transport of metal ions from the metal/semiconductor interface to the surface to form additional layers of oxide. This process will stop as the layer becomes thicker. For electron transfer via tunneling to be decisive, the oxide film cannot be a metal, because then it is not necessary to invoke tunneling as there are no band gaps that prohibit direct electronic communication. However, the ability of even a metallic, ultrathin oxide film, as it initially grows, to distort locally to accommodate charge that concomitantly will be stabilized by metallic screening may still be decisive for its chemical reactivity.

## SPECIFIC EXAMPLES

### Ultrathin Films Grown on Metal Supports

The most prominent example in the literature showing a pronounced SMSI effect via the formation of an oxide film overgrowing the metal particles is Pt/TiO<sub>2</sub> (10). Employing model systems, where Pt (as well as Pd) particles have been deposited onto TiO<sub>2</sub>(110) single crystal surfaces and annealed to elevated temperatures, it has been shown by scanning tunneling microscopy (STM) with atomic resolution that top facets of the Pt (Pd) particles are covered by a well-ordered, ultrathin oxide layer of a very complex structure (13, 14, 30–32). There is presently much debate about whether the structures observed are a complete titania layer or an intermetallic-like alloy. In addition, a large diversity of structures (including one observed on the titania-supported metal particles) were obtained in the course of growth of titania ultrathin films on Pt(111) (13, 32). Therefore, linking structure and reactivity for this system has to date been difficult. Instead, we address this issue by studying another model system, namely, Pt/Fe<sub>3</sub>O<sub>4</sub>(111), which features basically the same SMSI effect (33, 34).

It has been shown that annealing of Pt/Fe<sub>3</sub>O<sub>4</sub>(111) in vacuum at temperatures above 800 K causes Pt particle encapsulation by an iron oxide film, with the atomic structure virtually identical to a monolayer FeO(111) film grown on Pt(111) (**Figure 2**). It is well established that the FeO(111)/Pt(111) film consists of close-packed layers of Fe and O, stacked as O-Fe-Pt, and exhibits a Moiré pattern owing to the mismatch between the FeO(111) and Pt(111) lattices (35).

Once formed, this film is extremely stable and chemically inert under conditions typically applied in UHV-based experiments. It has turned out, however, that the film shows considerable CO oxidation activity when the reaction is performed at a millibar-range of pressures and relatively low temperatures (~450 K) (36), where Pt(111) is essentially inactive owing to the blocking effect

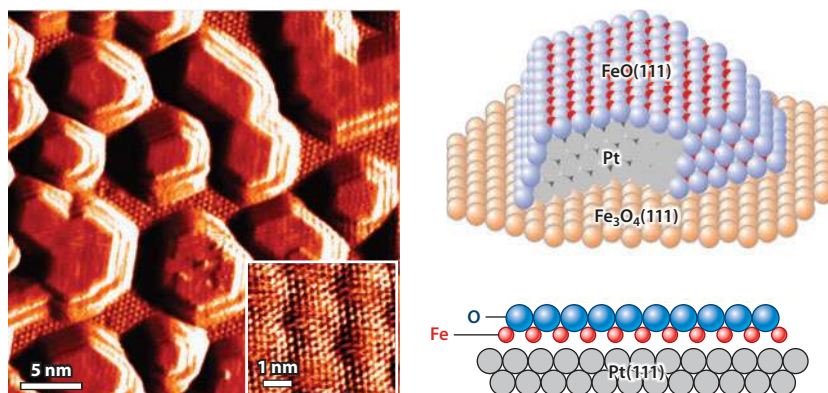


**Figure 2**

Scanning tunneling microscopy (STM) image (presented in the differentiated contrast) of Pt particles deposited onto  $\text{Fe}_3\text{O}_4(111)$  and annealed in vacuum at 850 K. An atomically resolved STM image of the top facet showing a 3-Å periodicity and long-range superstructure assigned to the formation of an  $\text{FeO}(111)$  layer on  $\text{Pt}(111)$  is shown in the inset. The structural models are shown at the right.

of CO on  $\text{O}_2$  dissociation (37). The experimental results were obtained by STM, Auger electron spectroscopy (AES), low-energy electron diffraction (LEED), and temperature-programmed desorption in combination with density functional theory (DFT) calculations and showed that at elevated pressures the bilayer  $\text{FeO}(111)$  film transforms into the trilayer O-Fe-O film, as shown in **Figure 3** (36, 38). The mechanism for this transformation includes  $\text{O}_2$  adsorption on the Fe atom pulled out of the pristine  $\text{FeO}$  film from the interface to the metal (**Figure 3a**). In this state, electrons are transferred from the oxide/metal interface to oxygen, resulting in a superoxo  $\text{O}_2^-$  species, which then dissociates, ultimately forming an O-Fe-O trilayer structure (**Figure 3b**). This reaction is computed to be site-specific within the Moiré unit cell, and as such may explain STM results showing the formation of close-packed  $\text{FeO}_2$  islands rather than a continuous  $\text{FeO}_2$  film (39).

The topmost oxygen atoms are more weakly bound than are those in the original  $\text{FeO}$  layer (38) and may readily react with incoming CO to form  $\text{CO}_2$  that leaves behind an oxygen vacancy upon desorption (**Figure 3c**). The overall activation barrier for  $\text{CO}_2$  formation, as determined by DFT ( $\sim 0.3$  eV), is considerably lower than the computed barrier for the CO oxidation reaction on  $\text{Pt}(111)$ , which is of the order of 1 eV (39, 42). Certainly, to end the catalytic cycle, the oxygen vacancies must be replenished via the reaction with  $\text{O}_2$  from the gas phase. Comparison of the  $\text{CO} + \text{O}_2$  and  $\text{CO} + \text{NO}$  reactions under the same conditions revealed that the replenishment of oxygen vacancies is the rate-limiting step that proceeds much faster with  $\text{O}_2$  than NO (40). As a result, the  $\text{CO} + \text{NO}$  reaction rate is negligible compared with  $\text{CO} + \text{O}_2$ .

Turning back to the encapsulated  $\text{Pt}/\text{Fe}_3\text{O}_4(111)$  system, in the light of structure and reactivity results obtained on the extended  $\text{FeO}(111)/\text{Pt}(111)$  films, one would reasonably expect higher reactivity of the encapsulated Pt particles as compared with the naked Pt particles. This was observed, indeed! Although the enhancement effect was found to be size-dependent (41), this finding indicated that the conclusions drawn for extended film surfaces could be extrapolated to finite-sized systems.

The results clearly show that it is the trilayer O-Fe-O film that catalyzes CO oxidation by providing weakly bound oxygen, whose formation occurs only at high oxygen pressures. It is important to note that both the transformation of the  $\text{FeO}$  into  $\text{FeO}_2$ -like film and the oxygen

**AES:** Auger electron spectroscopy

**LEED:** low-energy electron diffraction

**DFT:** density functional theory

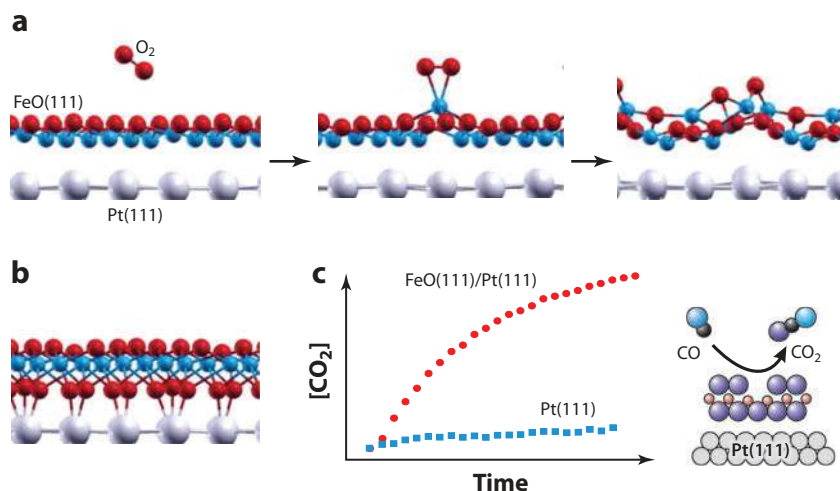


**Figure 3**

(a) Steps in transformation of bilayer FeO(111) into the trilayer O-Fe-O film at high O<sub>2</sub> chemical potentials as predicted by density functional theory. (b) Final structure. (c) Typical reaction kinetics of CO<sub>2</sub> production on FeO/Pt(111) and Pt(111) surfaces proceeding through a Mars-van Krevelen-like mechanism as depicted.

vacancy replenishment under the reaction conditions involve the charge transfer accompanied by a lattice distortion. As highlighted above, both factors favor the reaction on ultrathin films. Indeed, under the same conditions, the reaction proceeds with a much lower rate on thicker iron oxide Fe<sub>3</sub>O<sub>4</sub>(111) films (41).

Although in the case of O<sub>2</sub> interacting with the FeO layer on Pt, the O<sub>2</sub><sup>-</sup> species formed (in the course of the formation of the reactive FeO<sub>2</sub> trilayer) is a transient species, a stable O<sub>2</sub><sup>-</sup> species has been predicted to form on a thin MgO(100) layer on Ag(100) (42), which is then the active species in CO oxidation. The superoxo species is stabilized through polaronic distortion of the MgO lattice, which occurs only if the film is ultrathin. In fact, the polaronic distortion manifests itself in the *g*-tensor components of the electron paramagnetic resonance (EPR) signal, which may be directly compared with O<sub>2</sub><sup>-</sup> formed by a different mechanism on bulk MgO. This polaronic distortion is considerably smaller than that observed for FeO, which led to the transient species.

To verify the theoretical predictions, the interaction of the MgO(100) films with O<sub>2</sub> has recently been studied by EPR spectroscopy (43). The EPR results (Figure 4) revealed spontaneous activation of molecular oxygen forming an O<sub>2</sub><sup>-</sup> radical, which was observed only on very thin films and vanished upon increasing the film thickness to 15 monolayers (15 ML), i.e., in full agreement with the theoretical calculations. Note, however, that the reaction probability and the abundance of the O<sub>2</sub><sup>-</sup> formed are small; thus, it has not been possible so far to quantify the reactivity.

The reaction mechanism suggested for the MgO(100) films is hardly possible for the FeO/Pt system with its very high work function that renders the electron transfer to species on the film surface quite unlikely. In fact, the activation of oxygen initiating the FeO → FeO<sub>2</sub> transformation is only possible because of a local lowering of the work function by ~1.5 eV when the Fe cation is pulled out from the oxide/support interface into the top layer. Based on these considerations—and bearing in mind that for ultrathin films, the work function is basically determined by the substrate—one could, in principle, tune the reactivity of the oxide films by changing the metal support, provided that the oxide film grows with the same structure. The choice is not obvious per se because the growth of a particular oxide film is intimately related to its metal substrate.

EPR: electron  
paramagnetic  
resonance

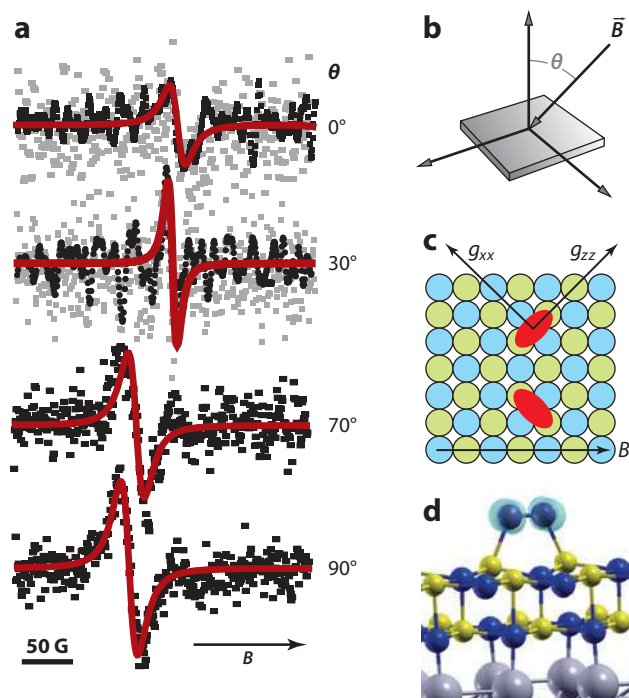


**Figure 4**

(a) Electron paramagnetic resonance spectra taken for 20 L O<sub>2</sub> (1 L = 10<sup>-6</sup> Torr sec) adsorbed at 30 K on a 4-ML thick MgO(001) film grown on Mo(001) as a function of the polar angle  $\theta$  (see panel *b* for definition). The magnetic field was oriented in a plane spanned by a direction equivalent to [100] in the surface and the surface normal. (c) Top view of the adsorption geometry (O<sub>2</sub> ovals, red; O, blue; Mg, green). (d) Calculated adsorption geometry (O, blue; Mg, green).

Following these ideas, we have recently initiated studies on iron oxide films grown on Pd(111), which has a lattice constant almost identical to that of Pt(111), i.e., 2.75 and 2.78 Å, respectively, but a considerably lower work function, i.e., 5.6 versus 6.1 eV. The prepared monolayer films on Pd(111) showed structural (LEED, AES, STM) characteristics (44) very similar to the FeO(111)/Pt(111) film. The films were then examined with respect to the CO oxidation reaction under the same reaction conditions (10 mbar CO + 50 mbar O<sub>2</sub> at 450 K) as studied previously on FeO/Pt(111) films. Again, the FeO(111) film on Pd(111) showed higher CO<sub>2</sub> production than did the bare Pd(111) surface, thus supporting the conclusion on the promotional effect of thin iron oxide films in low temperature CO oxidation. However, the observed rate enhancement was considerably lower than in the case of FeO(111)/Pt(111), which would sound counterintuitive if only considerations on work function were decisive. What do we expect based on the ideas presented above? On the one hand, the lower work function would facilitate the formation of O<sub>2</sub><sup>-</sup>. On the other hand, this may result in a stable O<sub>2</sub><sup>-</sup> species without alteration of the Fe-O stacking sequence, which is necessary for the formation of the reactive O-Fe-O film (**Figure 3a**). This, in turn, would lead to deactivation with respect to FeO/Pt(111) and might explain the observation, but certainly additional experimental studies are necessary to elucidate the atomic structure of the FeO/Pd films at elevated pressures.

One may notice that the O-Fe-O stoichiometry of the film implies Fe atoms in the formal oxidation state 4+, which is very uncommon for the iron oxides, and the DFT calculations actually

show that the oxidation state is close to 3+ owing to the presence of the metal substrate. Of course, there are transition metals that favor the required  $\text{MO}_2$  stoichiometry, e.g.,  $\text{MnO}_2$  and  $\text{TiO}_2$ , therefore their reactivity when prepared as ultrathin films may be of interest. The preparation of  $\text{MnO}_2$  films with the trilayer O-Mn-O structure has recently been reported on Pt(111) (45). Moreover, it has been shown that this film possesses more weakly bound oxygen than in the monolayer  $\text{MnO}(111)$  film, but reactivity has yet to be studied. The situation seems to be more complicated for ultrathin films of  $\text{TiO}_2$ , because several different, often coexisting, structures have been observed on Pt(111) (32). Nevertheless, the preparation of ultrathin oxide films is an extensively growing field, which makes expectations quite promising.

To sum up, the above examples demonstrate that ultrathin oxide films may enhance reactivity of metal catalysts, particularly in oxidation reactions in the low-temperature regime, where pure metal catalysts may suffer from site-blocking effects and strong chemisorption of reactants.

### Native Oxide Films on Metals

The above section dealt with oxide films of one metal grown on a substrate consisting of a second metal support. The next question is whether the same picture developed above holds true for native metal oxide films. In essence, there is nothing that would change the underlying physical principles. Under net oxidizing conditions and relatively high temperatures, even noble metals like Pt and Ag could, in principle, have surface oxide layers that may affect reactivity or even be the active phase in a reaction. Perhaps the most explored and still controversially discussed example concerns CO oxidation over ruthenium catalysts, which recently attracted the attention of the catalytic and surface science communities.

Considering model studies only, several oxygen-containing surface structures (**Figure 5**) have been suggested as the most active: (a)  $\text{O}(1 \times 1)\text{-Ru}(0001)$ , virtually formed only at high oxygen pressures; (b) a crystalline  $\text{RuO}_2(110)$  film approximately 1 nm in thickness on metallic  $\text{Ru}(0001)$ ; and (c) ill-defined transition surface oxides (16–24). Each model has its own pros and cons. It is fair to say that the experimental results critically depend on the surface preparation and reaction conditions (pressure, temperature,  $\text{CO/O}_2$  ratio). Mass transport effects bring additional complexity into such studies and become more critical at atmospheric pressures (46). Therefore, direct comparison of the results obtained in different research groups is often difficult if not impossible. It is generally believed that high catalytic activity is intimately connected with a disordered dynamic phase with significant compositional fluctuations. This conclusion is qualitatively similar but not as specific as the conclusions presented in the above section.

The initial stages of the oxide formation on  $\text{Ru}(0001)$  have been addressed by DFT (47). The results suggested that oxygen first occupies the surface hexagonal close-packed (hcp) sites in amounts up to 1 ML, and only then does the additional oxygen go subsurface, where it preferentially forms islands with a local  $(1 \times 1)$  periodicity and ultimately the hexagonal O-Ru-O structure (**Figure 6**). The total energy may be further minimized by a small lateral displacement (stretch) of the O-Ru-O layer that is relatively weakly coupled to the underlying metal. From a thermodynamic point of view, such a process could, in principle, be continued until a critical film thickness (equivalent to  $\sim 5$  ML of oxygen) was approached, where the transformation toward the more thermodynamically stable  $\text{RuO}_2(110)$  structure occurs.

To the best of our knowledge, systematic studies of the reactivity of  $\text{RuO}_x$  films as a function of the film thickness have not been performed. The study that comes closest is a low-energy electron microscopy study (48) on oxidation of  $\text{Ru}(0001)$  (albeit at low pressures) that indicated the coexistence of  $\text{RuO}_2(110)$  domains and a disordered, trilayer-like O-Ru-O-O surface oxide over a wide range of temperature and gas phase conditions, i.e., in variance to the previous view



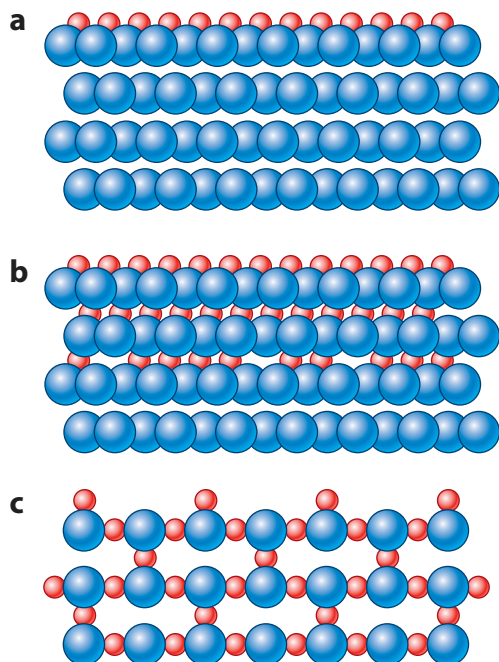


**Figure 5**

Schematic representation of the oxidation states of Ru(0001). (a) (1 × 1)-O adsorption phase with ~1 ML of oxygen; (b) transient surface oxides, RuO<sub>x</sub>, with oxygen incorporated into the subsurface layers; (c) rutile RuO<sub>2</sub>(110) phase.

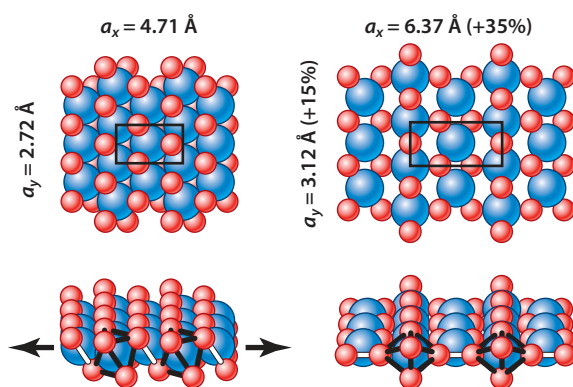


**Figure 6**

Atomic geometries of (a) the O-Ru-O trilayer and (b) the RuO<sub>2</sub>(110) structure. Top and perspective views are shown for both, with surface unit cells indicated. The rutile structure is achieved by expanding the trilayer in the directions indicated by the arrows. Adapted with permission from Reference 47. Copyright (2002), Elsevier.

**SXRD:** surface X-ray diffraction

**XPS:** X-ray photoelectron spectroscopy

on surface oxides as a metastable precursor to the RuO<sub>2</sub>(110) thin-film oxide. Both structures rapidly and uniformly react with CO and can be reoxidized in O<sub>2</sub>. This behavior was taken as an indication of high CO oxidation activity, which was shown to be much higher than that observed on a (1 × 1)-O phase.

There is still debate over which is the more active phase and at what temperature, but all groups agree that the binding energy of oxygen species involved in the reaction has to be sufficiently small to render the system active. So far, reaction theory models have considered CO oxidation only on the stoichiometric RuO<sub>2</sub>(110) surface and not on ultrathin films. Neither has the process of creating the trilayer film as well as the stoichiometric surface been investigated. Therefore, a direct comparison of mechanisms occurring on the O-Fe-O and O-Ru-O films is not possible at present.

This ruthenium puzzle triggered a closer look and more elaborative studies on other platinum group metal catalysts operating in oxygen ambient. Certainly, ruthenium has a much higher affinity to oxygen as compared to the noble metal catalysts, e.g., Rh, Pd, and Pt, that are widely used in oxidation of exhaust gases, volatile organic compounds, etc. Indeed, dissociative adsorption energies of oxygen are of 334, 234, 230, and 188 kJ mol<sup>-1</sup> for the close-packed Ru, Rh, Pd, and Pt surfaces, respectively, which correlates with standard heats of formation for RuO<sub>2</sub>, Rh<sub>2</sub>O<sub>3</sub>, PdO, and PtO<sub>2</sub> (-153, -119, -116, and -71 kJ mol<sup>-1</sup>, respectively) (49). Although the formation of surface oxide films on Rh, Pd, and Pt in the oxygen ambient is less favorable, it is not impossible per se at the high chemical potential of oxygen. Several studies have recently been reported on the oxidation of noble metals, in particular, for the more open surfaces such as (100) and (110), which are known to be far more reactive to oxygen than (111). These studies are surveyed below.

Employing STM inside a high-pressure flow reactor allowed in situ recording of the morphology of the Pt(110) surface and its reactivity in CO oxidation (50). Switching from CO to O<sub>2</sub> flow (0.5 bar, 425 K) and back caused reversible extensive roughening of the Pt surface that was interpreted in terms of the formation of a thin platinum oxide film accompanied by high CO<sub>2</sub> production, presumably through a Mars-van Krevelen mechanism. According to DFT studies (51) that followed the initial experimental investigations, the surface oxides on Pt(110) are metastable and must be stabilized, e.g., by defects and/or kinetic restrictions.

Further in situ studies using surface X-ray diffraction (SXRD) (52) suggested that under O<sub>2</sub>-rich conditions in the temperature range of 425–625 K, the surface is covered with the α-PtO<sub>2</sub>-like oxide film, with a nominal thickness corresponding to the 2–3 stacks of an O-Pt-O triple layer. [Note also that trilayer α-PtO<sub>2</sub> structures have very recently been reported for the Pt(111) surface, but their formation is kinetically limited, indeed (53)]. The oxide film is either distorted compared with bulk α-PtO<sub>2</sub> to accommodate the Pt(110) surface or it exhibits totally incommensurate structures. The commensurate oxide appeared only when both O<sub>2</sub> and CO were present in the reaction ambient at sufficiently high temperatures. This finding was explained by DFT in terms of a stabilization effect of chemisorbed carbonate ions. Importantly, both oxides showed substantially higher catalytic activity than the metallic Pt surface.

On Pd(111), two-dimensional oxides were observed, even at low oxygen pressures, as intermediate phases between an oxygen overlayer and bulk PdO (54). Further STM, SXRD, X-ray photoelectron spectroscopy (XPS), and DFT studies (55) suggested the formation of an incommensurate surface oxide of Pd<sub>3</sub>O<sub>4</sub> stoichiometry and almost coplanar geometry that has no resemblance to any bulk oxides of Pd.

The oxidation of the Pd(100) surface at low O<sub>2</sub> pressures proceeds through several steps, ultimately resulting in either a (5 × 5)- or a (√5 × √5)R27°-ordered structure, depending on the experimental conditions, both originally assigned to the single PdO layer (56). Surprisingly, the latter structure [essentially a strained PdO(101) trilayer on Pd(100) (57)] has been observed even at 575 K and 1 bar O<sub>2</sub> in the course of SXRD studies of CO oxidation over Pd(100) at elevated

pressures (58). The formation of an  $\sim 4$ -nm-thick, poorly ordered bulk oxide phase with predominantly PdO(001) orientation occurred primarily at higher temperatures. A significant discrepancy between the experimental and the DFT-computed stability phase diagram was rationalized on the basis of kinetic hindrance to the formation of the bulk oxide.

Again, as in the case of Pt(110), the in situ STM studies (59) at atmospheric pressures revealed morphological changes from adsorbate-covered Pd(100) to an oxidic state depending on the CO:O<sub>2</sub> ratios. However, unlike the Pt(110) surface, where roughening was shown to be reaction-induced, the Pd(100) surface became rough upon oxidation. The CO oxidation was accompanied by further surface roughening. In the oxidic state, the surface showed a considerably higher reactivity, which was proposed to proceed via the Mars–van Krevelen mechanism.

A temperature-programmed reaction study in the  $10^{-8}$ – $10^{-6}$  mbar pressure range revealed that the  $(\sqrt{5} \times \sqrt{5})R27^\circ$  surface was essentially inert in CO oxidation (56). The bulk-like PdO overlayer was even less reactive to CO. The low reactivity of these structures was tentatively assigned to their inability to strongly adsorb CO. Combined with the technique of temperature-programmed reaction, the in situ STM and LEED results suggested that upon exposure to CO, the  $(\sqrt{5} \times \sqrt{5})R27^\circ$  structure transforms into the much more active  $(2 \times 2)$  structure, which probably contains subsurface oxygen. The results indicated that the inactive structures in fact supply oxygen for replenishing those structures from the  $(2 \times 2)$  domains.

Nevertheless, as the best-established structure of a Pd-oxide layer on Pd, the  $(\sqrt{5} \times \sqrt{5})R27^\circ$  surface has been considered in a DFT analysis of CO oxidation on Pd(100) (60). The results suggested that the monolayer oxide film might indeed be a relevant structure for the CO oxidation reaction on Pd(100) at technologically relevant pressures. Further first-principles kinetic Monte Carlo simulations revealed that local pressure and temperature fluctuations may induce a continuous formation and decomposition of oxidic phases during steady-state reaction such that both oxidic and reduced states become important for the reaction.

Finally, well-ordered ultrathin oxide films form on Rh surfaces (61–63). In particular, the combination of high-resolution XPS, STM, SXRD, and DFT revealed the self-limited growth of an O–Rh–O trilayer film on Rh(111) at intermediate oxygen pressures (61). The film forms a coincidence superstructure very similar to FeO(111)/Pt(111), as depicted in **Figure 7**. However, based on the DFT results, this surface oxide is only a transient, kinetically stabilized structure. A thick,

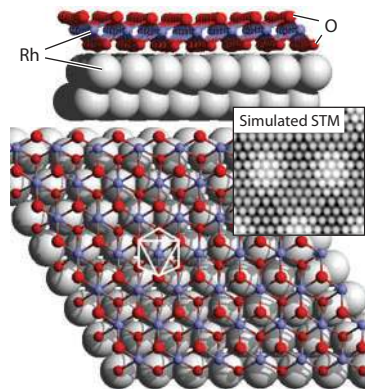


**Figure 7**

Side and top views of the most stable O–Rh–O surface oxide as calculated by density functional theory. A simulated scanning tunneling microscopy (STM) image is shown in the inset. Reprinted with permission from Reference 61. Copyright (2004) by the American Physical Society.

corundum-like  $\text{Rh}_2\text{O}_3$  bulk oxide, which is thermodynamically more stable, forms at significantly higher pressures and temperatures, e.g., 10 mbar and 800 K. Interestingly, the similar O-Rh-O films were observed on Ru(100) and even on highly stepped Rh(553) and Rh(223) surfaces, where the original step structure of the metal single crystal completely vanished upon oxidation (63).

Recent combined SXRD and reactivity (mass spectrometry) studies of the Rh(111) surface provided strong evidence that the trilayer surface oxide is much more active than is metallic Rh in low-temperature ( $\sim 500$  K) CO oxidation, whereas the Rh bulk oxide was not active at all (62). Although, from their experiments, the authors could not rule out the possibility that it was the combination of the surface oxide and the metallic surface that was responsible for the highest reactivity results, there is definitely a close similarity in the structure-reactivity relationship between the  $\text{RhO}_2/\text{Rh}$  and the previously discussed  $\text{FeO}_2/\text{Pt}$  systems.

### CONCLUDING REMARKS

Ultrathin metal oxide films turn out to exhibit interesting properties. Although in the past, oxide films covering metal surfaces were considered detrimental for catalysis, as suggested by the observation of the SMSI-induced encapsulation of metal particles on the reducible oxide supports. With the culmination of recent evidence, there are also clear indications that oxide overlayers may enhance activity for CO oxidation over the supporting metal. The mechanism of formation of the active oxide film is not evident in all cases, but it seems that the formation of rather weakly bound oxygen is a crucial factor in rendering the oxide film active under reaction conditions. Although in most cases, a clear identification of the details of formation and reaction of the active film has not been possible, the case of FeO on Pt has allowed us to unravel the mechanism of formation of the active film, its structure, and the rate-determining step in CO oxidation. In most other cases, experimental and theoretical studies have concentrated on structural aspects of various phases formed and not on the mechanism of formation and structural change under reaction conditions. We believe that a continuously growing body of studies on structure and reactivity of ultrathin oxide films in conjunction with potentially interesting target reactions could ultimately result in an avenue leading to the rational design of the monolayer oxidation catalysts, which are in essence metal-supported monolayer oxides. This is equivalent to a concept that has been put forward several decades ago (64, 65) without having the tools at hand to prove it.

#### SUMMARY POINTS

1. Ultrathin oxide films may be grown on metal supports, from either the same or a different metal representing the support.
2. Ultrathin films are flexible with respect to their structure and respond to external stimuli, including the chemical potential of the gas phase they are exposed to.
3. Due to the combination of geometric structures and the concomitant electronic structures, thin oxide films may be used to control charge transfer from the metal support to adsorbed species and thus trigger chemical reactions.
4. Combinations of surface analytical techniques allow the direct investigation of structure-reactivity relations for ultrathin oxide films and the identification of the active phase formed in situ.
5. The processes involved in active phase formation may be described following ideas put forward in early theories of metal oxidation.

## DISCLOSURE STATEMENT

The authors are not aware of any affiliations, memberships, funding, or financial holdings that might be perceived as affecting the objectivity of this review.

## ACKNOWLEDGMENTS

We thank Gianfranco Pacchioni and Paul Bagus for many useful discussions on theory and Niklas Nilus, Thomas Risse, as well as Martin Sterrer for participating in part of the research reviewed. We are grateful to the German Science Foundation for support through Sonderforschungsbereich 546 and the Cluster of Excellence “Unifying Concepts in Catalysis.” The Fonds der Chemischen Industrie is acknowledged for financial support.

## LITERATURE CITED

1. Freund H-J. 2010. Model studies in heterogeneous catalysis. *Chem. A Eur. J.* 16:9384
2. Freund H-J, Pacchioni G. 2008. Oxide ultra-thin films on metals: new materials for the design of supported metal catalysts. *Chem. Soc. Rev.* 37:2224
3. Freund H-J. 2002. Clusters and islands on oxides: from catalysis via electronics and magnetism to optics. *Surf. Sci.* 500:271
4. Campbell CT. 2006. Transition metal oxides: extra thermodynamic stability as thin films. *Phys. Rev. Lett.* 96:066106
5. Libuda J, Freund H-J. 2005. Molecular beam experiments on model catalysts. *Surf. Sci. Rep.* 57:157
6. Nilus N, Risse T, Schauerer S, Shaikhtudinov S, Sterrer M, Freund H-J. 2011. Model studies in catalysis. *Top. Catal.* 54:4
7. Tauster SJ, Fung SC, Garten RL. 1978. Strong metal-support interactions. Group 8 noble metals supported on titanium dioxide. *J. Am. Chem. Soc.* 100:170
8. Ko EI, Garten RL. 1981. Ethane hydrogenolysis of TiO<sub>2</sub>-supported group VIII metal catalysts. *J. Catal.* 68:233
9. Knözinger H, Taglauer E. 2008. Wetting and spreading. In *Handbook of Heterogeneous Catalysis*, ed. G Ertl, H Knözinger, F Schüth, J Weitkamp, p. 555. Berlin: Wiley-VCH. 2nd ed.
10. Tauster SJ. 1987. Strong metal-support interaction. *Acc. Chem Res.* 20:389
11. Haller G, Resasco DE. 1989. Metal-support interactions between Group VIII metals and reducible oxides. *Adv. Catal.* 36:173
12. Bernal S, Calvino JJ, Cauqui MA, Gatica JM, Larese C, et al. 1999. Some recent results on metal/support interaction effects in NM/CeO<sub>2</sub> (NM: noble metal) catalysts. *Catal. Today* 50:175
13. Wu Q-H, Fortunelli A, Granozzi G. 2009. Preparation, characterisation and structure of Ti and Al ultrathin oxide films on metals. *Int. Rev. Phys. Chem.* 28:571
14. Dulub O, Hebenstreit W, Diebold U. 2000. Imaging cluster surfaces with atomic resolution: the strong metal-support interaction state of Pt supported on TiO<sub>2</sub>(110). *Phys. Rev. Lett.* 84:3646
15. Netzer FP, Allegretti, Surnev S. 2010. Low-dimensional oxide nanostructures on metals: hybrid systems with novel properties. *J. Vac. Sci. Technol. B* 28:doi: 10.1116/1.3268503
16. Peden CHF, Goodman DW. 1986. Kinetics of CO oxidation over Ru(0001). *J. Phys. Chem.* 90:1360
17. Stampfl C, Scheffler M. 1997. Anomalous behavior of Ru for catalytic oxidation: a theoretical study of the catalytic reaction CO + 1/2 O<sub>2</sub> → CO<sub>2</sub>. *Phys. Rev. Lett.* 78:1500
18. Over H, Kim YD, Seitsonen, Wendt S, Lundgren E, et al. 2000. Atomic-scale structure and catalytic reactivity of the RuO<sub>2</sub>(110) surface. *Science* 287:1474
19. Goodman DW, Peden CHF, Chen MS. 2007. CO oxidation on ruthenium: a brief history of bridging the gaps. *Surf. Sci.* 601:L124
20. Narkhede V, Afmann J, Muhler M. 2005. Structure-activity correlations for the oxidation of CO over polycrystalline RuO<sub>2</sub> powder derived from steady-state and transient kinetic experiments. *Z. Phys. Chem.* 219:979



21. Blume R, Hävecker M, Zafeiratos S, Teschner D, Kleimenov E, et al. 2006. Catalytically active states on Ru(0001) catalyst in CO oxidation reaction. *J. Catal.* 239:354
22. Over H, Balmes O, Lundgren E. 2009. In situ structure-activity correlation experiments of the ruthenium catalyzed CO oxidation reaction. *Catal. Today* 145:236
23. Gao F, Wang Y, Cai Y, Goodman DW. 2009. CO oxidation over Ru(0001) at near-atmospheric pressures: from chemisorbed oxygen to RuO<sub>2</sub>. *Surf. Sci.* 603:1126
24. Reuter K. 2006. Insight into a pressure and materials gap: CO oxidation at “ruthenium” catalysts. *Oil Gas Sci. Technol.* 61:471
25. Bell A. 2003. The impact of nanoscience on heterogeneous catalysis. *Science* 299:1688
26. Schalow T, Brandt B, Starr DE, Laurin M, Shaikhutdinov SK, et al. 2006. Size-dependent oxidation mechanism of supported Pd nanoparticles. *Angew. Chem. Int. Ed.* 45:3693
27. Nelin CJ, Bagus PS, Brown MA, Sterrer M, Freund H-J. 2011. Analysis of the broadening of X-ray photoelectron spectroscopic peaks for ionic crystals. *Angew. Chem. Int. Ed.* In press
28. Pacchioni G, Giordano L, Baistrocchi M. 2005. Charging of metal atoms on ultrathin MgO/Mo(100) films. *Phys. Rev. Lett.* 94:226104
29. Cabrera N, Mott NF. 1948. Theory of the oxidation of metals. *Rep. Prog. Phys.* 12:163
30. Bowker M, Stone P, Morrall P, Smith R, Bennett R, et al. 2005. Model catalyst studies of the strong metal-support interaction: surface structure identified by STM on Pd nanoparticles on TiO<sub>2</sub>(110). *J. Catal.* 234:172
31. Bowker M. 2007. Catalysis resolved using scanning tunneling microscopy. *Chem. Soc. Rev.* 36:1656
32. Barcaro G, Agnoli S, Sedona F, Rizzi GA, Fortunelli A, Moruzzi G. 2009. Structure of reduced ultrathin TiO<sub>x</sub> polar films on Pt(111). *J. Phys. Chem. C* 113:5721
33. Qin Z-H, Lewandowski M, Sun Y-N, Shaikhutdinov S, Freund H-J. 2008. Encapsulation of Pt nanoparticles as a result of strong metal-support interaction with Fe<sub>3</sub>O<sub>4</sub>(111). *J. Phys. Chem. C* 112:10209
34. Qin Z-H, Lewandowski M, Sun Y-N, Shaikhutdinov S, Freund H-J. 2009. Morphology and CO adsorption on Pt supported on thin Fe<sub>3</sub>O<sub>4</sub>(111) films. *J. Phys. Condens. Matter* 21:134019
35. Weiss W, Ranke W. 2002. Surface chemistry and catalysis on well-defined epitaxial iron-oxide layers. *Prog. Surf. Sci.* 70:1
36. Sun Y-N, Qin Z-H, Lewandowski M, Carrasco E, Sterrer M, et al. 2009. Monolayer iron oxide film on platinum promotes low temperature CO oxidation. *J. Catal.* 266:359
37. Imbihl R, Ertl G. 1995. Oscillatory kinetics in heterogeneous catalysis. *Chem. Rev.* 95:697
38. Sun Y-N, Giordano L, Goniakowski J, Lewandowski M, Qin Z-H, et al. 2010. The interplay between structure and CO oxidation catalysis on metal supported ultrathin oxide films. *Angew. Chem. Int. Ed.* 49:4418
39. Giordano L, Lewandowski M, Groot I, Sun Y-N, Goniakowski J, et al. 2010. The oxygen-induced transformations of a FeO(111) film on Pt(111): a combined DFT and STM study. *J. Phys. Chem. C* 114:21504
40. Lei Y, Lewandowski M, Sun Y-N, Fujimori Y, Martynova Y, et al. 2011. CO+NO versus CO+O<sub>2</sub> reaction on monolayer FeO(111) films on Pt(111). *ChemCatChem* 3:671
41. Lewandowski M, Sun Y-N, Qin Z-H, Shaikhutdinov S, Freund H-J. 2011. Promotional effect of metal encapsulation on reactivity of iron oxide supported Pt catalysts. *Appl. Catal. A* 391:407
42. Hellman A, Klacar S, Grönbeck H. 2009. Low temperature CO oxidation over supported ultrathin MgO films. *J. Am. Chem. Soc.* 131:16636
43. Gonchar A, Risse T, Freund H-J, Giordano L, Di Valentin C, et al. 2011. Activation of oxygen on MgO: O<sup>2-</sup> radical ion formation on thin, metal supported MgO(001) films. *Angew. Chem. Int. Ed.* 50:2635
44. Sun YN. 2010. *Enhanced reactivity of ultrathin oxide films in oxidation reactions: back to “electronic theory of catalysis.”* PhD thesis. Free Univ., Berlin. 145 pp.
45. Sachert S. 2008. *Bestimmung der vibratorischen, thermischen und strukturellen Eigenschaften von Manganoxiden auf Pt(111) mittels HREELS, TPD und LEED.* PhD thesis. Martin Luther Univ., Halle-Wittenberg, Ger. 103 pp.
46. Matera S, Reuter K. 2010. Transport limitations and bistability for in situ CO oxidation at RuO<sub>2</sub>(110): first-principles based multiscale modeling. *Phys. Rev. B* 82:085446
47. Reuter K, Stampfl C, Ganduglia-Pirovano MV, Scheffler M. 2002. Atomistic description of oxide formation on metal surfaces: the example of ruthenium. *Chem. Phys. Lett.* 352:311



48. Flege JI, Hrbek J, Suter P. 2008. Structural imaging of surface oxidation and oxidation catalysis on Ru(0001). *Phys. Rev. B* 78:165407
49. Chen MS, Cai Y, Yan Z, Gath KK, Axnanda S, Goodman DW. 2007. Highly active surfaces for CO oxidation on Rh, Pd and Pt. *Surf. Sci.* 601:5326
50. Hendriksen BLM, Frenken JWM. 2002. CO oxidation on Pt(110): scanning tunneling microscopy inside a high-pressure flow reactor. *Phys. Rev. Lett.* 89:046101
51. Li WX, Österlund L, Vestergaard, EK, Vang, RT, Matthiesen J, et al. 2004. Oxidation of Pt(110). *Phys. Rev. Lett.* 93:146104
52. Ackermann MD, Pedersen TM, Hendriksen BLM, Robach O, Bobaru SC, et al. 2005. Structure and reactivity of surface oxides on Pt(110) during catalytic CO oxidation. *Phys. Rev. Lett.* 95:255505
53. Krasnikov SA, Murphy S, Berdunov N, McCoy AP, Radican K, Shvets IV. 2010. Self-limited growth of triangular PtO<sub>2</sub> nanoclusters on the Pt(111) surface. *Nanotechnology* 21:335301
54. Zheng G, Altman EI. 2000. The oxidation of Pd(111). *Surf. Sci.* 462:151
55. Lundgren E, Kresse G, Klein C, Borg M, Anderson JN, et al. 2002. Two-dimensional oxide on Pd(111). *Phys. Rev. Lett.* 88:246103
56. Zheng G, Altman EI. 2002. The reactivity of surface oxygen phases on Pd(100) toward reduction by CO. *J. Phys. Chem. B* 106:1048
57. Todorova M, Lundgren E, Blum V, Mikkelsen A, Gray S, et al. 2003. The Pd(100)-( $\sqrt{5} \times \sqrt{5}$ )R27°-O surface oxide revisited. *Surf. Sci.* 541:101
58. Lundgren E, Gustafson J, Mikkelsen A, Andersen JN. 2004. Kinetic hindrance during the initial oxidation of Pd(100) at ambient pressures. *Phys. Rev. Lett.* 92:046101
59. Hendriksen BLM, Babaru SC, Frenken JWM. 2004. Oscillatory CO oxidation on Pd(100) studied with in situ scanning tunneling microscopy. *Surf. Sci.* 552:229
60. Rogal J, Reuter K, Scheffler M. 2008. CO oxidation on Pd(100) at technologically relevant pressure conditions: first-principles kinetic Monte Carlo study. *Phys. Rev. B* 77:155410
61. Gustafson J, Mikkelsen A, Borg M, Lundgren E, Köhler L, et al. 2004. Self-limited growth of a thin oxide layer on Rh(111). *Phys. Rev. Lett.* 92:126102
62. Gustafson J, Westerström R, Mikkelsen A, Torrelles X, Balmes O, et al. 2008. Sensitivity of catalysis to surface structure: the example of CO oxidation on Rh under realistic conditions. *Phys. Rev. B* 78:045423
63. Gustafson J, Resta A, Mikkelsen A, Westerström R, Andersen JN, Lundgren E. 2006. Oxygen-induced step bunching and faceting of Rh(553): experiment and ab initio calculations. *Phys. Rev. B* 74:035401
64. Vol'kenshtein FF. 1966. Experiment and the electronic theory of catalysis. *Russ. Chem. Rev.* 35:537
65. Schwab G-M. 1978. Electronics of supported catalysts. *Adv. Catal.* 27:1

